Optical Model for Proton Scattering from ^{40}Ca

G. L. Thomas and B. C. Sinha
Wheatstone Laboratory, King's College, Strand, London, WC2R 2LS, England
(Received 4 September 1970)

A six-parameter optical model for proton elastic scattering from ^{40}Ca has been developed in which the real part of the potential has been generated from a matter distribution that reproduces the single-particle binding energies and electron elastic-scattering cross sections. A Gaussian nucleon-nucleon force has been used and an optimum range of 4.5 ± 0.4 fm^2 extracted. Improved fits are obtained with a density-dependent effective interaction.

The reformulated optical model of Greenlees, Pyle, and Tang[1] has been used successfully to describe proton elastic scattering from a range of nuclei under the assumption of a Woods-Saxon shape for the matter distribution. Since the parameters of the matter distribution are varied to fit the data it is not possible to obtain information on the two-body force. The aim of the present work is to use matter distributions known to reproduce experimental binding energies, single-particle levels, and electron-scattering data, to generate an optical potential and to examine its sensitivity to various effective interactions, by fitting proton elastic-scattering data for ^{40}Ca. We have taken matter distributions from various nuclear structure calculations[2-5] for use in our model, the potential for which has the form

$$U_{\mathrm{opt}}(r) = V_c(r) - VI(r)/I(0) - iW_v f(r, r_I, a_I) + iW_D 4a_I \frac{d}{dr} f(r, r_I, a_I) + V_s \left(\frac{\hbar}{m_\pi c}\right)^2 \frac{1}{r}\frac{d}{dr}\rho_m(r)\vec{\sigma}\cdot\vec{l}, \tag{1}$$

where $V_c(r)$ is the potential due to a uniformly charge sphere of radius $R_c = r_c A^{1/3}$, $f(r, r_I, a_I)$ is a Woods-Saxon form factor, and $\rho_m(r)$ is the matter distribution, and with

$$\begin{aligned} I(r) &= \int \rho_n(\vec{r}')t_{pn}(|\vec{r}-\vec{r}'|)d^3r' + \int \rho_p(\vec{r}')t_{pp}(|\vec{r}-\vec{r}'|)d^3r' \\ &= \int [\rho_n(\vec{r}')+\rho_p(\vec{r}')]\tfrac{1}{2}[t_{pn}(|\vec{r}-\vec{r}'|)+t_{pp}(|\vec{r}-\vec{r}'|)]d^3r' + \int [\rho_n(\vec{r}')-\rho_p(\vec{r}')]\tfrac{1}{2}[t_{pn}(|\vec{r}-\vec{r}'|)-t_{pp}(|\vec{r}-\vec{r}'|)]d^3r' \\ &= \int \rho_m(\vec{r}')u_d(|\vec{r}-\vec{r}'|)d^3r' + \int \rho_{ne}(\vec{r}')u_\tau(|\vec{r}-\vec{r}'|)d^3r', \end{aligned} \tag{2}$$

where $t_{pn}(r)$ and $t_{pp}(r)$ are respectively the proton-neutron and proton-proton parts of the effective interaction and $\rho_{ne}(r) = \rho_n(r) - \rho_p(r)$ is the neutron excess distribution. For ^{40}Ca the latter is nearly zero so we are concerned only with the first term in Eq. (2). We use two types of effective interaction, a Gaussian of the form $u_d(r) = \exp(-kr^2)$ and a density-dependent force known to take into account the state dependence of the two-body interaction. We use the Green form[6] of the density-dependent effective interaction with

$$t_{pp}(r) = \tfrac{1}{4}V_s(r), \quad t_{pn}(r) = \tfrac{1}{8}[V_s(r) + 3V_t(r)],$$

where s and t refer to the singlet-even and triplet-even parts of the interaction and

$$V_{s,t}(r) = c_{s,t}(1 - a_{s,t}\rho^{2/3}|\vec{r}+\vec{r}'|/2)V_{s,t}^{\mathrm{KK}},$$

where $V_{s,t}^{\mathrm{KK}}$ is the Kallio-Kolltveit potential[7] specified by

$$V_{s,t}^{\mathrm{KK}}(r) = V_{s,t}\exp(-k_{s,t}r) \text{ for } r > d_{s,t};$$
$$= 0 \text{ for } r \leq d_{s,t}.$$

A recent modification of the reformulated model[8] has shown that inclusion of terms in the spin-orbit part other than the first-order term used here does not improve the fit, so they have been omitted in this model. Our model does not include explicitly small effects due to antisymmetrization or core polarization, except in their simulation by the use of density dependence. Once the mean square radius ($\langle r^2\rangle_d = 3/2k$) of the Gaussian nucleon-nucleon force has been determined there are six variable parameters, V, W_v, W_D, V_s, r_I, and a_I, whichever effective interaction is used.

We have analyzed the proton-scattering data of Ridley and Turner[9] and Craig et al.[10] at 30 MeV, Fricke et al.[11] at 40 MeV, and Gross et al.[12] at 35.8 and 45.5 MeV. For a preliminary evaluation we analyzed the 35.8-MeV data with $\langle r^2\rangle_d = 4$ fm^2 for the nucleon-nucleon form factor. Three different matter distributions were used[3-5] and when the six parameters were optimized it was found that the model was unable to differentiate between them, in visual quality of fit or χ^2 (see Table I). Since the Negele distribution[5] gave the best fit and is probably superior on physical grounds, this was used in all subsequent analy-

Table I. Optical-model parameters obtained in fitting ^{40}Ca proton elastic-scattering data.

E_p	V	W_v	W_D	r_I	a_I	V_s	$\rho_m(r)$	$u_d(r)$	χ^2
35.8	56.8	4.0	0.7	1.63	0.50	25.4	ref.3	G(4)[a]	3003
"	56.2	4.1	0.8	1.61	0.48	23.8	ref.4	G(4)[a]	3040
"	57.6	4.0	0.5	1.67	0.46	25.5	ref.5	G(4)[a]	2715
"	56.9	3.6	1.0	1.63	0.51	25.0	"	G(4.5)[a]	2936
"	51.4	3.3	1.9	1.52	0.59	25.1	"	WDD	2367
"	47.4	2.6	2.3	1.50	0.63	24.5	"	SDD	2759
30.3	61.0	3.9	-1.3	2.00	0.50	25.8	"	G(4.5)[a]	2163
"	54.9	3.9	-1.3	2.02	0.56	26.0	"	WDD	2391
"	51.0	3.8	0.6	1.75	0.38	27.3	"	SDD	2151
40.0	56.5	4.9	0.0	1.62	0.59	25.4	"	G(4.5)[a]	2890
"	51.1	5.6	-1.7	1.81	0.86	23.8	"	WDD	2739
"	46.7	4.6	1.4	1.44	0.64	24.0	"	SDD	2165
45.5	56.2	5.0	0.1	1.63	0.34	28.3	"	G(4.5)[a]	2929
"	49.0	4.3	0.3	1.66	0.41	25.3	"	WDD	2410
"	44.4	7.5	-2.6	1.68	0.91	26.5	"	SDD	2028

[a]Denotes Gaussian form factor, with mean square radius as indicated.

sis. Using this distribution an investigation was carried out to determine the optimum $\langle r^2\rangle_d$. All six parameters were varied for a range of values of $\langle r^2\rangle_d$ and the best fits were obtained at 4.8 ± 0.8, 4.2 ± 1.0, 4.8 ± 1.6, and 4.1 ± 1.5 fm^2, at 30, 35, 40, 45 MeV, respectively. The errors have been assigned on the basis of a factor of 1.5 increase in χ^2 from the minimum, so the value of $\langle r^2\rangle_d$ is well determined, particularly at the lower energies where the data are more accurate. In the modified, reformulated optical model[8] the quantity $\langle r^2\rangle_d$ is not determined because of the larger number of degrees of freedom. The consistency of the values of $\langle r^2\rangle_d$ around the mean of 4.5 ± 0.4 fm^2 (standard deviation) strengthens the validity of this approach. The optimum fits to the data with the Gaussian effective interaction with $\langle r^2\rangle_d = 4.5$ fm^2 are shown in Figs. 1 and 2, along with the optimum fits for a thirteen-parameter optical model that includes a surface-derivative term in the real potential.[13]

We used both the weak (WDD) and strong (SDD) prescriptions for the density-dependent effective interaction and the best fits obtained are also shown in Figs. 1 and 2 and the resulting parameters in Table I. In all cases better fits could be obtained with some form of density dependence with improvements in χ^2 to about $\frac{2}{3}$ of the best-fit value with a Gaussian form factor at the higher energies. The differences in the best-fit angular distributions for the three effective interactions become more pronounced as the incident proton energy increases, so that by 45.5 MeV the differences are quite dramatic. It is evident that, provided the nuclear matter distribution is known, proton elastic scattering is sensitive to the form of the two-body interaction in nuclei.

We have also calculated an effective mean square radius $\langle r^2\rangle_{2n}$ for the density-dependent two-body effective interaction where, following Slanina and McManus,[14]

$$\langle r^2\rangle_{2n} = \langle r^2\rangle_{rc} - \langle r^2\rangle_m,$$

where $\langle r^2\rangle_{rc}$ and $\langle r^2\rangle_m$ are the mean-square radii of the real central potential and matter distributions, respectively. We found $\langle r^2\rangle_{2n} = 3.8$ fm^2 (SDD) and 4.4 fm^2 (WDD) which agree quite well

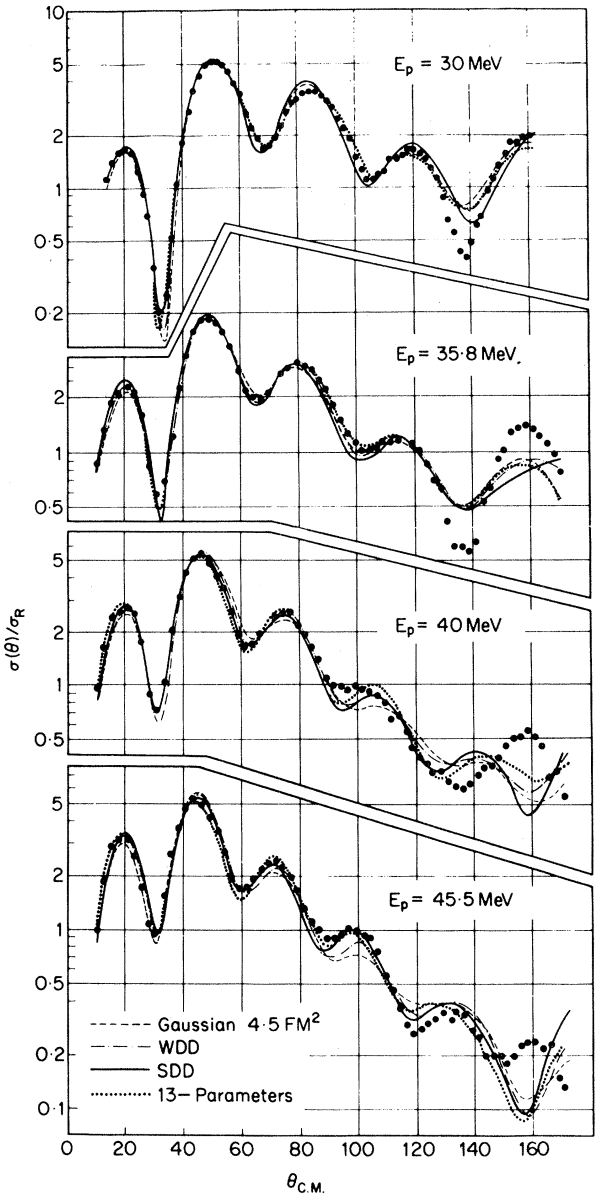

FIG. 1. Fits to the differential cross-section data for ^{40}Ca using the model defined by Eq. (1) for various effective interactions and for a thirteen-parameter optical model (Ref. 13).

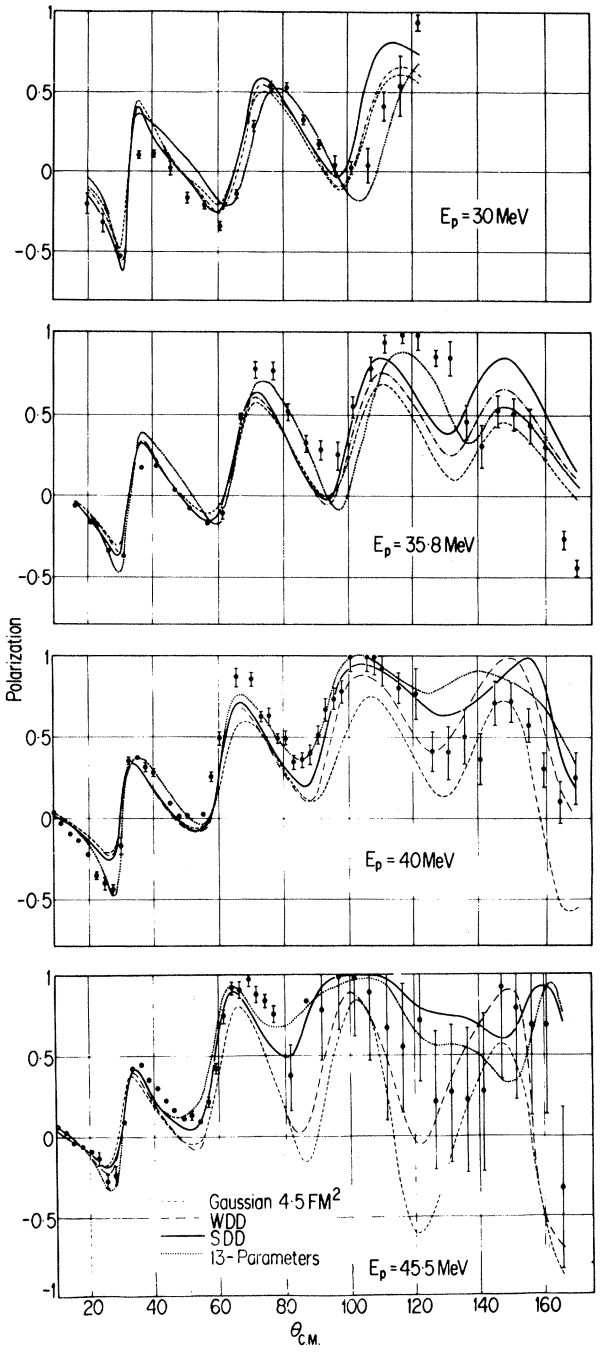

FIG. 2. Fits to the polarization data that correspond to the differential cross-section fits of Fig. 1.

with the value of 4.5 fm^2 obtained with the Gaussian form factor, thus confirming that the effective mean square radius is a well-determined quantity, within this model.

It is worth noting that this model tends to favor a larger absorption radius than the conventional model and often we obtain a negative value for the surface-absorption depth W_D. The latter feature is due to a surface-volume ambiguity: It was found that fits of similar quality, particularly at the higher energies, could be obtained without surface absorption.

We conclude that our six-parameter model, generated from a matter distribution that reproduces the experimental binding energies, single-particle energies, and electron-scattering cross sections, is satisfactory in describing proton elastic scattering and that, with the matter dis-

tribution known, the model is sensitive to the type of nucleon-nucleon interaction incorporated.

The authors wish to thank Professor L. R. B. Elton for useful discussion; Dr. C. J. Batty, Dr. H. S. Kohler, and Dr. J. W. Negele for furnishing us with the matter point densities for ^{40}Ca; and Dr. A. Zucker for sending unpublished data.

[1]G. W. Greenlees, G. J. Pyle, and Y. C. Tang, Phys. Rev. 171, 1115 (1968).
[2]A. Swift and L. R. B. Elton, Phys. Rev. Lett. 17, 484 (1966).
[3]C. J. Batty and G. W. Greenlees, Nucl. Phys. A133, 673 (1969).
[4]H. S. Kohler, Nucl. Phys. A139, 353 (1969).
[5]J. W. Negele, Phys. Rev. C 1, 1260 (1970).
[6]A. M. Green, Phys. Lett. 24B, 384 (1967).
[7]A. Kallio and K. Kolltveit, Nucl. Phys. 53, 87 (1964).
[8]G. W. Greenlees, W. Makofske, and G. J. Pyle, Phys. Rev. C 1, 1145 (1970).
[9]B. W. Ridley and J. F. Turner, Nucl. Phys. 58, 497 (1964).
[10]R. M. Craig *et al.*, Nucl. Phys. 58, 513 (1964).
[11]M. P. Fricke, E. E. Gross, B. J. Morton, and A. Zucker, Phys. Rev. 156, 1207 (1964).
[12]E. E. Gross *et al.*, Nucl. Phys. A102, 673 (1967).
[13]B. C. Sinha and V. R. W. Edwards, Phys. Lett. 31B, 273 (1970).
[14]D. Slanina and H. McManus, Nucl. Phys. A116, 271 (1968).

Small-Angle j Dependence of (α, p) Reactions*

J. E. Glenn,† C. D. Zafiratos, and C. S. Zaidins
Department of Physics and Astrophysics, University of Colorado, Boulder, Colorado 80302
(Received 12 November 1970)

We have observed the small-angle j dependence of (α, p) reactions for $l=1$ and $l=2$ reactions. The small-angle effect appears to persist for cases where the large-angle j dependence is small or absent.

Both distorted-wave Born-approximation (DWBA) calculations and rather general geometrical considerations predict a small-angle j dependence for (α, nucleon) reactions.[1] The results of Ref. 1 are that an appropriately weighted average of the $j=l+\frac{1}{2}$ and the $j=l-\frac{1}{2}$ angular distributions will give the angular distribution expected for no spin-orbit interactions and, further, they predict that near 0° the $j=l+\frac{1}{2}$ cross section will drop relative to that for the $j=l-\frac{1}{2}$. The magnitude of the effect will depend on spin-orbit strengths but the sign is unique. A previous small-angle study of (α, t) reactions indicated small effects,[2] presumably due to a small spin-orbit force in the triton optical potential.[3,4]

To test the small-angle prediction we studied two reactions proceeding to $l=1$ states where both the $j=\frac{3}{2}$ and $j=\frac{1}{2}$ states were observable. These were ^{12}C$(\alpha,p)^{15}$N and ^{62}Ni$(\alpha,p)^{65}$Cu. Further, we studied the reactions ^{26}Mg$(\alpha,p)^{29}$Al and ^{28}Si$(\alpha,p)^{31}$P proceeding to levels with $l=2$, $j=\frac{5}{2}$ and $\frac{3}{2}$. These reactions were observed at bombarding energies of 28 and 35.5 MeV. Protons were detected by conventional ΔE-E counter-telescope methods at angles greater than 15° while small-angle data were obtained with an absorber foil in front of a single semiconductor detector. Overlapping points obtained with both methods gave good agreement. The absorber

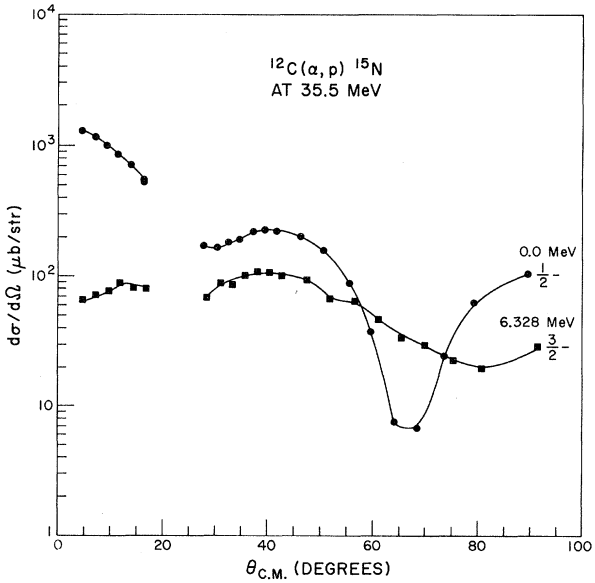

FIG. 1. Angular distributions for the $p_{1/2}$ (0.0-MeV) level and the $p_{3/2}$ (6.328-MeV) level of ^{15}N. The curves serve only to guide the eye. The upper j state shows filling in of minima and a significant drop (compared to the lower j state) at small angles.